IEEE Access
Multidisciplinary ⋮ Rapid Review ⋮ Open Access Journal

Received January 28, 2021, accepted February 2, 2021, date of publication February 8, 2021, date of current version February 24, 2021.

Digital Object Identifier 10.1109/ACCESS.2021.3058004

Antenna Array for Ku-Band MIMO GB-SAR

ANWER S. ABD EL-HAMEED [1,2], (Member, IEEE), AND MOTOYUKI SATO [1], (Fellow, IEEE)
[1]Center for Northeast Asian Studies, Tohoku University, Sendai 980-8576, Japan
[2]Electronics Research Institute, Giza 12622, Egypt

Corresponding author: Anwer S. Abd El-Hameed (ahmed.anwer.sayed.abdelhameed.b6@tohoku.ac.jp)

ABSTRACT A new multi-input multi-output (MIMO) antenna configuration with wideband and low sidelobe level (SLL) is introduced for ground-based synthetic aperture radar (GB-SAR). The proposed MIMO antenna has 15 transmitting and 16 receiving antenna arrays, arranged in two parallel straight lines, to synthesize a virtual array of 256 elements suitable for monitoring relatively large areas. The inter-element spaces are optimized to λ between transmitting elements and 4λ between receiving elements, to realize both low mutual coupling and an inferior SLL of lower than −37 dB for the overall MIMO antenna. The MIMO antenna element has eight rectangular patch linear arrays working at 17.1 GHz. A traveling wave-feeding network with center excitation is used to feed each element, in order to reduce the SLL and achieve a wide bandwidth of more than 300 MHz. The antenna array shows a gain of 14.3 dBi and half-power beamwidths (HPBWs) of 10° and 105° in the elevation and azimuth planes, respectively. The performance of the proposed design satisfies the GB-SAR requirements, which are validated by fabrication and measurement.

INDEX TERMS Array antenna, GB-SAR, MIMO, patch antenna.

I. INTRODUCTION

The development of devices that aid ground surface disaster prevention is in great demand worldwide, particularly in countries that experience unstable environmental changes such as earthquakes, rainfall, and severe weather. Ground-based synthetic aperture radar (GB-SAR) has been used effectively to measure ground surface displacements [1]–[5]. A conventional GB-SAR system comprises transmitting and receiving horn antennas sliding on a metal bar to cover the required synthetic aperture. The size and weight of the system are significant drawbacks, especially in transportation [6]–[8]. The rapid data acquisition of GB-SAR has a vital role in assessing swiftly changing atmospheric effects, and it can be employed to measure the vibrations of large structures [9].

Recently, multi-input multi-output (MIMO) radar has attracted much attention as an alternative to the mechanical GB-SAR [10]–[17]. The development of new MIMO antenna configurations for radar systems to monitor large areas is demanded. In [13] a MIMO radar was constructed with 4 × 4 horn antennas operating at the X-band. A 6 × 6 folded dipole MIMO antenna working at the C-band was used to configure a MIMO radar to synthesize an equally spaced virtual array of 36 elements [16]. A 2 × 6 planar MIMO antenna with coaxial cavity horn elements was used to construct a MIMO radar system with great area coverage [17]. All these researches employed horn antennas as transmitting and receiving sensors, and they occupy large areas. Furthermore, the synthesized aperture is still too small and is insufficient for use over large observation areas.

Planar antennas offer low cost, low weight, and very modest geometry [18]–[20]. Various simple techniques can be used to provide high gain when compared to the horn antennas commonly used in GB-SAR devices [21]–[24]. Usually, antenna arrays comprise individual elements fed by a feeding network. To control an antenna array's radiation properties, the feeding network and the arrangement of array elements must be designed thoughtfully. There are various techniques for enhancing the patch antenna bandwidth [25]. Stacked dielectrics and metallic vias are often used, making the antenna design complicated and unreliable.

This paper introduces a simple alternative MIMO antenna configuration based on the patch antenna, replacing the movable horn antenna of a commercial Ku-band GB-SAR. Its antenna elements are based on a traveling wave-feeding network, which provides broad bandwidth and low cross-radiation to strengthen element isolation. The proposed antenna has the advantages of stationarity, good radiation performance, light weight, low cost, and a large synthetic

The associate editor coordinating the review of this manuscript and approving it for publication was Di Zhang.

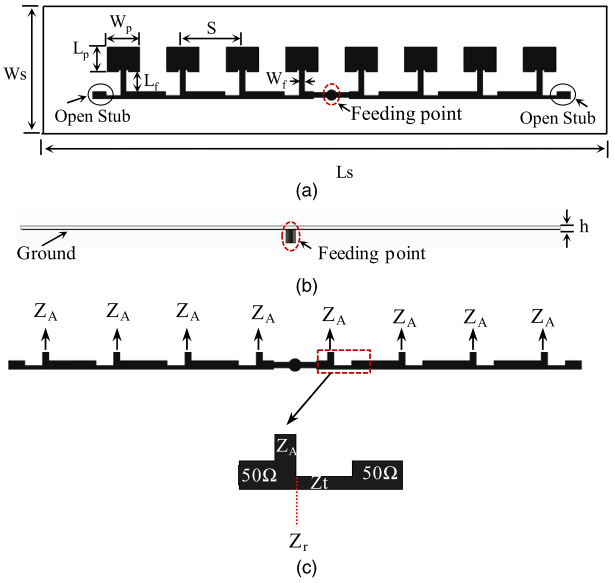

FIGURE 1. Antenna array geometry. (a) Top view (b) Side view (c) Feeding network.

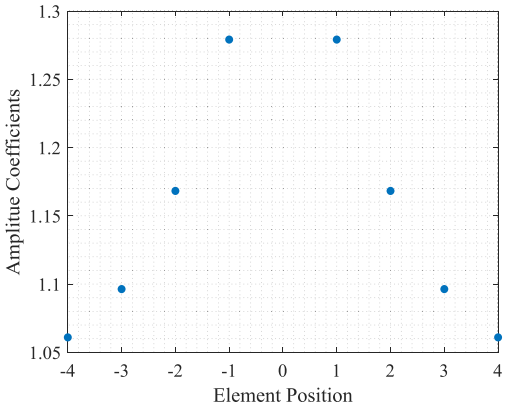

FIGURE 2. Amplitude coefficients distribution along the array elements.

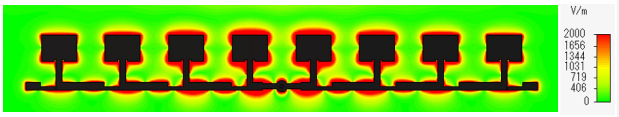

FIGURE 3. Electric field distribution.

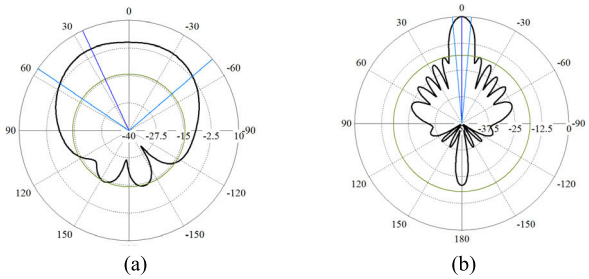

FIGURE 4. Radiation pattern at 17.1 G Hz. (a) Azimuth-Plane. (b) Elevation-plane.

aperture. It consists of 15 transmitting and 16 receiving antennas aligned parallel to each other to synthesize 256 equally-spaced "virtual elements" with a high gain of 14.3 dBi and a sidelobe level (SLL) lower than −37 dB. The developed antenna was assembled with other GB-SAR components and tested, showing outstanding performance. Electromagnetic CST software was used for antenna simulations.

II. ANTENNA DESIGN

The conventional GB-SAR is a portable transceiver device operating in the Ku-band [10]. Lightweight printed antennas are recommended due to their use of new features. The antenna gain requirements depend on the distance between the target and the system. Commonly, the nominal gain value varies from 10 dB to 20 dB. The 3 dB beamwidth is the most significant parameter for GB-SAR transceiver antennas, which should be narrow in the azimuth plane and wide in the elevation plane. A narrow beamwidth in the elevation plane will reduce ground clutter and will boost the signal to noise ratio (SNR). A wide azimuth beamwidth improves illumination of the observation area. Accordingly, our goal is to design an antenna ranging from 17.1 GHz to 17.25 GHz and with half-power beamwidths (HPBWs) of 105° and 10° in the azimuth and elevation planes, respectively. The proposed MIMO antenna configuration comprises 31 elements: 15 transmitters and 16 receivers. Each transmitter and receiver element is composed of a linear antenna array to help reach the desired requirements.

A. DESIGN OF MIMO ELEMENT

Fig. 1 illustrates the structure of a linear antenna array centrally excited by a traveling wave-feeding network. The proposed array consists of 2N elements. In the traveling wave-feeding technique, the impedance of the patches is matched with the impedance at the central feeding point of the feeding network, as well as the point where the patch joins the feeding network. It is able to maintain the desired radiation pattern, unlike a resonant array, which introduces many more possibilities for deterioration of the radiation pattern. In addition, the traveling wave-feeding structure offers a fairly wide bandwidth and high efficiency, which preferable for remote sensing applications. Two λg/2 open circuit stubs are added to the array to reflect the power traveling toward the ends. The amplitude distribution at each array element is extracted using (1).

$$|A_i| = k^{i-1} + k^{2N-i}, i = 1, \ldots .N, \tag{1}$$

where k is the coefficient which determines the amount of power feeding each radiating element. It can be calculated using (2).

$$k = 1 - \frac{Z_o}{Z_A}, \tag{2}$$

where Z_o is the main feeding line's characteristic impedance, which is 50 Ω, and Z_A is the patch antenna impedance at its feeder, as shown in Fig. 1(b). It should be noted that the second term in (1) expresses the reflected power from

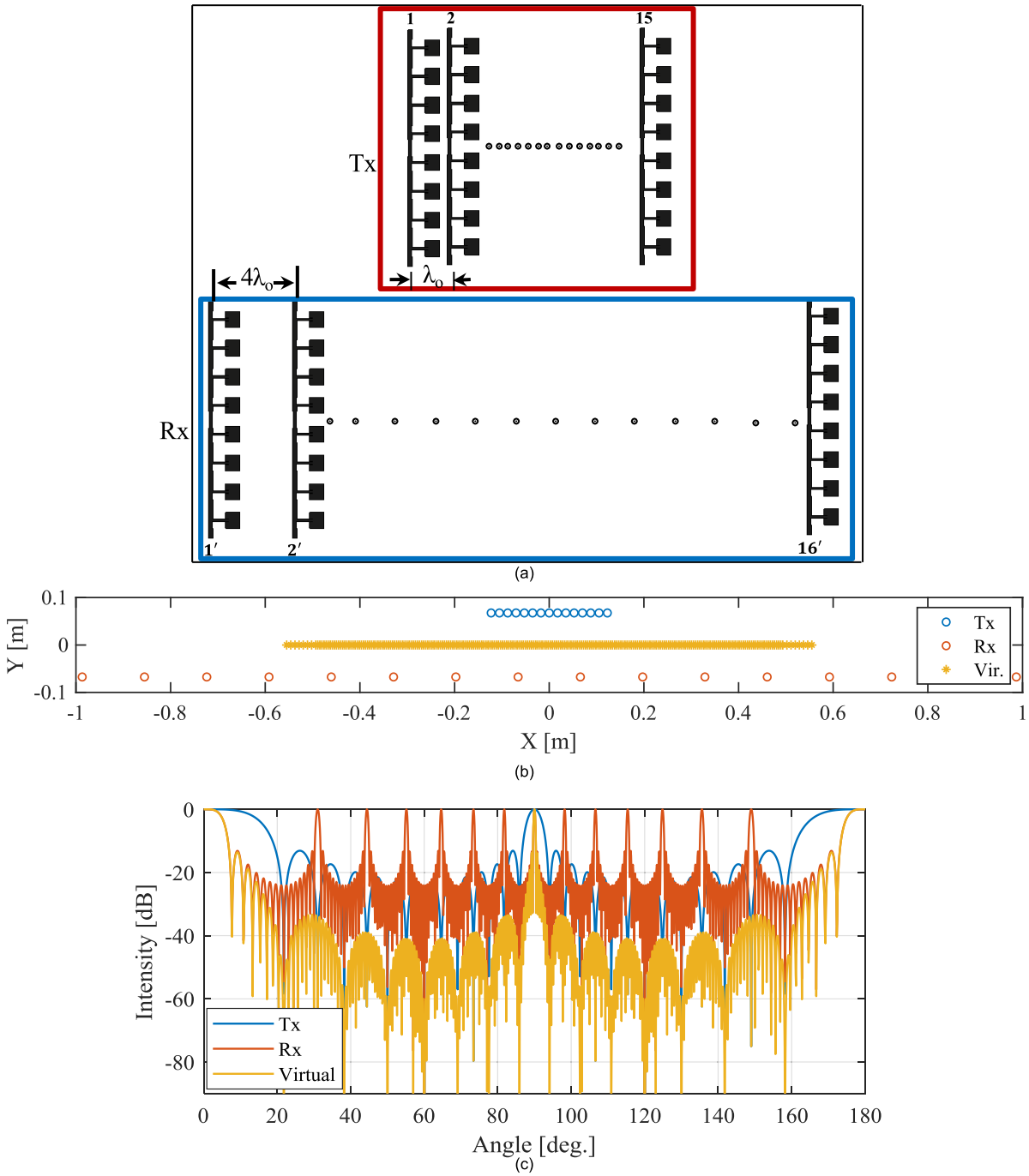

FIGURE 5. MIMO antenna configuration. (a) Transmitting and receiving antenna arrangement. (b) Virtual array distribution. (c) Normalized Array factor for Tx, Rx and MIMO.

the λg/2 open circuit stub. Hence, the returned power arrives at the feeding point in phase. The optimizing of k is carried out using EM-CST software, and $k = 5/6$ is selected as the optimum value because it shows the highest suppression of SLL.

The rectangular patch antenna is chosen as a main radiating element of the antenna array. An impedance of $Z_A = 300\Omega$ is selected to satisfy the optimized k value. The impedance of the patch in parallel to the impedance at the reference $Z_r = 60\Omega$ provides exactly the characteristic impedance of the microstrip line, which is 50Ω. By matching the feeding line impedance of 50Ω to the quarter-wave transformer impedance, $Z_t = 54.8\Omega$, an impedance of 60Ω can be attained, as shown in Fig. 1(c). The distance between each radiating element is set at λg. To validate the effect of the optimum k value, the amplitude distribution along the prospective antenna array and the electric field distribution are illustrated in Fig. 2 and Fig. 3, respectively. The electric field is symmetrically distributed on both sides with reference to the center feeding point, showing a lower concentration in

TABLE 1. Antenna geometrical parameters (unit: mm).

L_s	W_s	L_p	W_p	L_f	W_f	S	h
110	12.7	4.5	6.01	3.9	1	10.9	0.6

the border elements and contributing to SLL reduction. The proposed antenna array is designed on the PPE substrate, with $\varepsilon_r = 3.3$, $\tan\delta = 0.003$, and h = 0.6 mm. Table 1 sets out the dimensions of the proposed antenna structure.

Fig. 4 shows the antenna radiation pattern in both azimuth and elevation planes. The antenna obtained a high gain of 14.3 dBi, with HPBWs of 10° and 105° in the elevation and azimuth planes, respectively, and a SLL of −18.5 dB. The traveling wave-feeding technique helped to achieve the required antenna specification.

B. DESIGN OF MIMO ARRAY

We arranged only 31 elements (15 transmitters and 16 receivers) to synthesize a virtual array of 256 elements, as shown in Fig. 5(a). We selected this number of elements as it is suitable for monitoring relatively large areas. Assume a MIMO antenna operating with a central wavelength λ, and suppose the transmitting antennas are placed in positions x_m, where m varies from 1 to 15, and the receiving antennas are placed in positions y_l, where l varies from 1 to 16. Consider a target placed at a distance $r\bar{e}$ from the radar system. The equivalent MIMO array factor FMIMO(e), which is commonly known as the array factor of the virtual array, is derived by multiplying the transmitting array factor F_{Tx} by the receiving array factor F_{Rx}, as expressed in (3).

$$F_{MIMO}(e) = F_{TX}(e)F_{TX}(e) = \frac{1}{N}e^{i\frac{4\pi}{\lambda}r}\sum_{m,l}\left(e^{\left(\frac{xm+yl}{2}\right).e}\right) \tag{3}$$

To attain a low SLL for the MIMO configuration, FTX is recommended to be null at every FRX grating lobe, and vice versa. Accordingly, the separation between any two consecutive elements is chosen to be λ_0 for Tx and $4\lambda_o$ for Rx. Fig. 5(b) shows the typical array factor of the proposed configuration. It is obvious that the virtual array SLL is below −37 dB along the most effective illumination angle, from 20° to 160°, due to the F_{RX} grating lobe cancellation by the F_{TX} nulls.

III. EXPERIMENTAL RESULTS

A. ANTENNA RESULTS

To authenticate the introduced MIMO configuration for practical use, the 15 transmitting elements and 16 receiving elements were fabricated and attached to one metal sheet, ready to serve in a radar system, as shown in Fig. 6. The measured and simulated S-parameters are depicted in Fig. 7, indicating perfect agreement. The measured S-parameters show an operating bandwidth of more than 400 MHz, covering the desired bandwidth from 17.1 GHz to 17.52 GHz. The measured isolation between transmitter #7 and receiver #8, which are

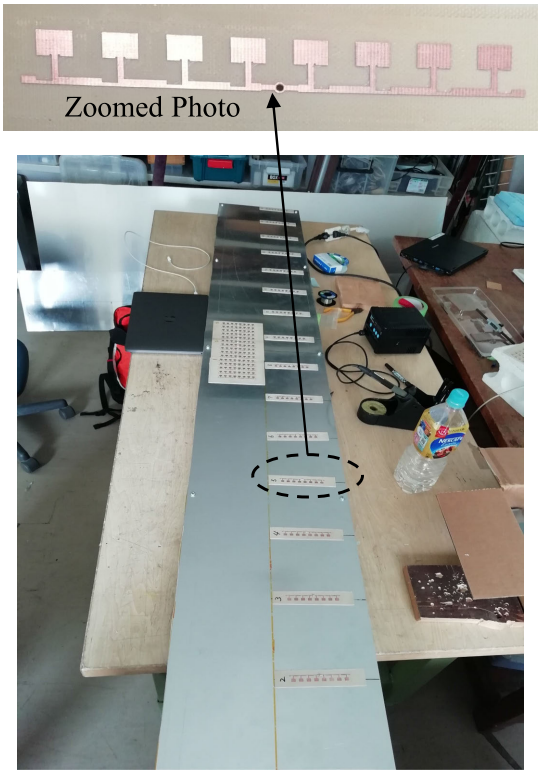

FIGURE 6. Fabricated prototype of the proposed MIMO antenna.

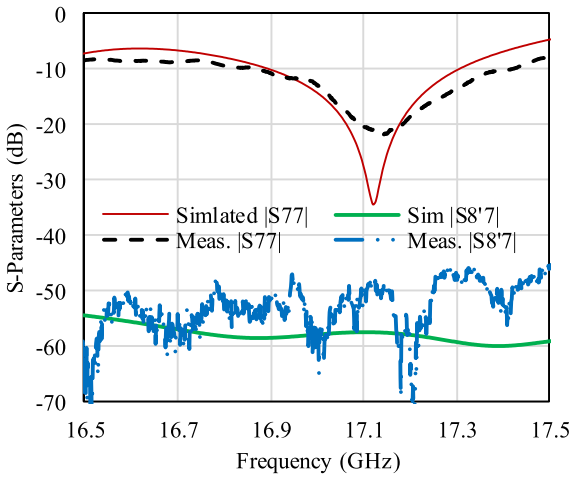

FIGURE 7. Measured and simulated reflection coefficient.

closest to each other, is also better than −45 dBi, which is excellent for MIMO performance.

Moreover, various parameters should be studied to evaluate the proposed MIMO antenna performance, such as envelope correlation coefficient (ECC) and diversity gain. The ECC is one of the main parameters that evaluate multi-antenna systems performance; it illustrates how far the MIMO channels are isolated or correlated with each other. There are two ways for ECC calculations: radiation pattern based and S-Parameters based, assuming the antenna elements are lossless and well-matched. Due to the fatiguing of using the radiation pattern for the ECC computation, the S-parameters

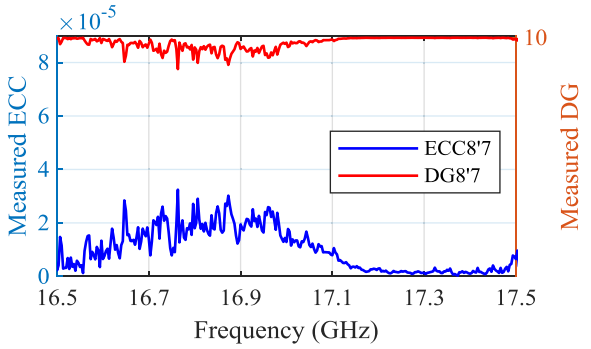

FIGURE 8. Measured envelope correlation coefficient and diversity gain.

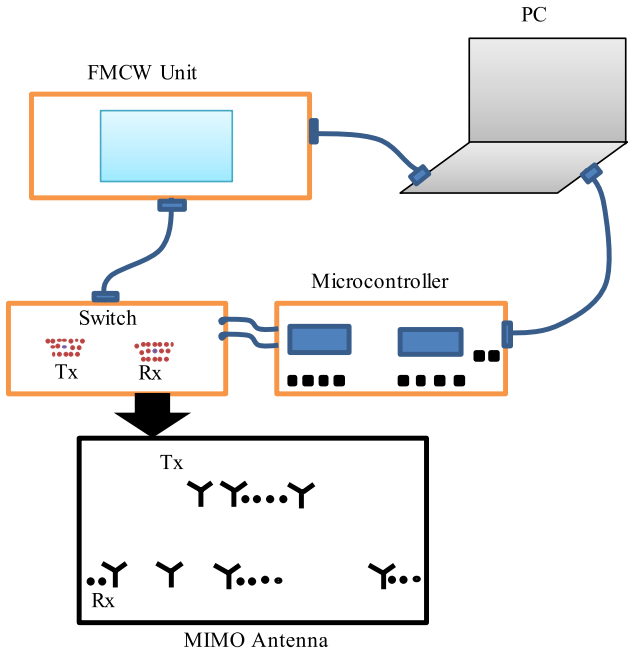

FIGURE 9. Block diagram of the MIMO GB-SAR.

based method is favored. For the two-element antenna system, the ECC can be formulated by (4):

$$\rho_e = |\rho_{ij}| = \frac{\left|S_{ii}^* S_{ij} + S_{ji}^* S_{jj}\right|^2}{(1 - (|S_{ii}|^2 + |S_{ji}|^2))(1 - (|S_{jj}|^2 + |S_{ij}|^2))} \tag{4}$$

Fig. 8 describes the measure ECC between transmitter #7 and receiver #8. It is seen that the ECC through the whole band is less than 4×10^{-5} and these values satisfy the criteria of the ECC condition for MIMO system.

Diversity gain represents the improvement in the performance of the antenna in terms of its signal to noise ratio using diversity techniques. It can be calculated using (5). Fig. 8 shows that the measured diversity gain is almost 10 dB across the whole band.

$$DG = 10\sqrt{1 - (ECC)^2} \tag{5}$$

Finally, in Table 2, the performance of the proposed antenna is compared to the most recent research. Our

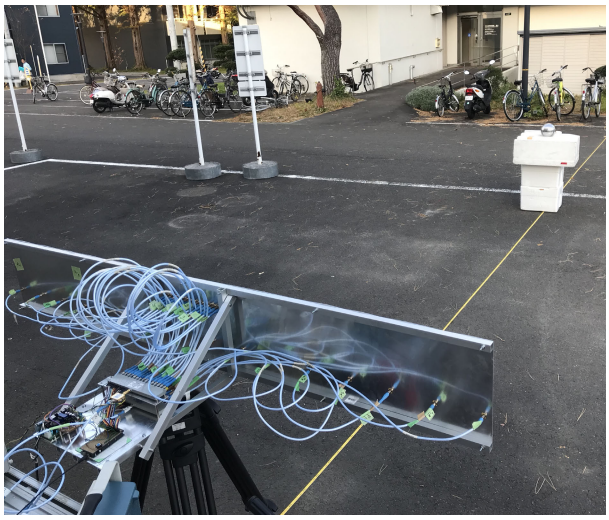

FIGURE 10. Experiment setup.

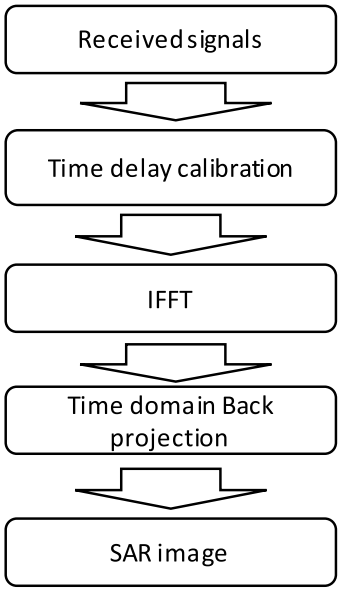

FIGURE 11. Signal processing flowchart.

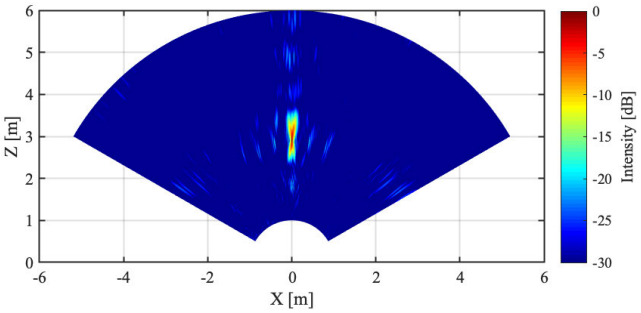

FIGURE 12. SAR image of sphere target.

proposed MIMO antenna has the highest gain, narrowest elevation HPBW, widest azimuth HPBW, and simplest structure. The number of transmitting and receiving elements is the highest, with the exception of [27]. However, our proposed

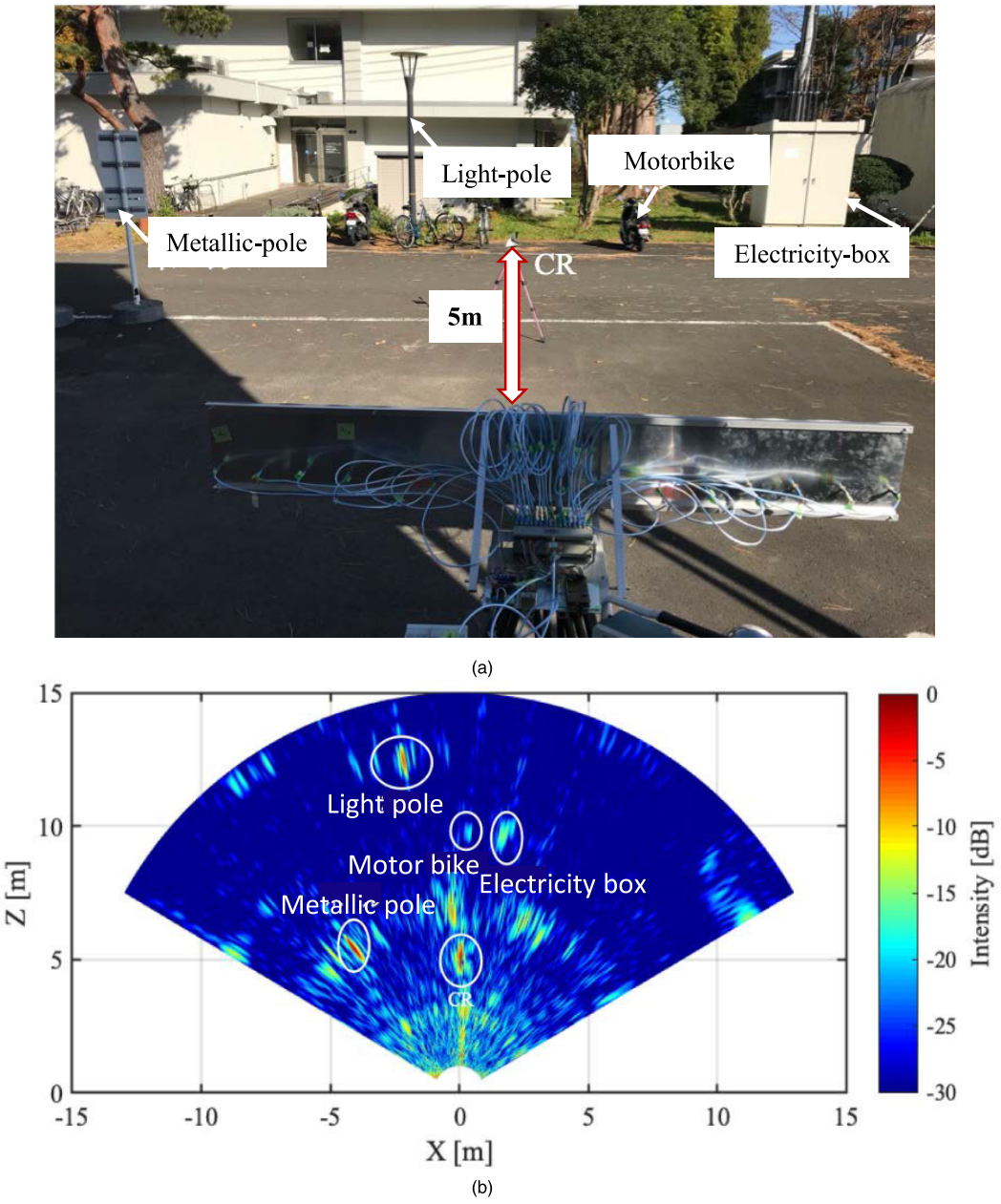

FIGURE 13. Outdoor experiment. (a) Experiment setup. (b) Corresponding SAR image.

antenna is superior in gain and radiation pattern characteristics. It can provide the largest synthetic aperture, making it very suitable for most GB-SAR applications. The exploitation of highly integrated microstrip technology makes it cheaper than other technologies of coaxial cables and horn antennas. Additionally, new applications can be accommodated that are beyond the scope of a conventional GB-SAR, such as the measurement of vibration in structures, due to the speed of data acquisition of MIMO technology.

B. RADER VALIDATION

A radar prototype was used to validate the proposed MIMO antenna structure for GB-SAR imaging, as shown in Fig. 9. The distance between transmitting antennas is 17 mm and the distance between receiving antennas is 68 mm, as discussed in the previous section. This arrangement produces 256 virtual elements, uniformly spaced. The frequency-modulated continuous wave (FMCW) unit works as a transceiver. An Arduino device controls the switching system. The FCMW signal is transmitted to the Tx switch stage and the transmitted signal is then transferred to the 15 transmitting antenna elements. The reflected signal is received by the receiving antennas, governed by the Rx switch. The data are then passed through an analog to digital converter, and finally acquired by a PC.

The performance of the MIMO radar with the proposed antenna was tested using a metallic sphere of 10 cm diameter as a target. It was placed 3 m from the radar antenna, as shown

TABLE 2. Performance comparison of the proposed mimo configuration with other state-of-the-art work.

Ref	Element Type	Number of Elements	Operating Band	HPBW (Azimuth, Elevation) in [Deg.]	Gain [dB]
[13]	Horn Antenna	4×4	X-Band	NG	10
[16]	Folded Dipole	6×6	C-Band	NG	NG
[26]	Stacked Structure of Patch Antenna	4×6	Ku-Band	30^0 , 16^0	11.2
[17]	Coaxial Cavity Horn Antenna	2×6	Ku-Band	104.8^0, 26.21^o	10.24
[27]	Stacked Patch antenna	16×16	X-Band	80^0 , 60^0	13.6 including PA
This Work	Linear Patch array	15×16	Ku-band	105^o, 10^o	14.3

in Fig. 10. The signal processing flowchart we used to obtain a two-dimensional SAR image is shown in Fig. 11. The time delay through cables, switches, the FCMW unit, and the antenna positions' tolerance were calibrated. After the delay calibration, we removed the background by subtracting data both with and without the target. The back-projection algorithm was used to reconstruct the SAR image. Fig. 12 shows the SAR images, which indicate very low clutter. These results reveal that the proposed antenna configuration has a very low SLL, as discussed in the previous section.

Furthermore, the radar azimuth resolution was examined by identifying several reflecting targets at various ranges and azimuth angles. Accordingly, the system has been deployed in an outdoor environment, as shown in Fig. 13 (a). Moreover, we placed a corner reflector 5 m from the radar antenna, as a reference. Fig. 13 (b) shows the ability of our antenna to recognize the surrounding targets. The successful target detection proves that the GB-SAR based on our MIMO structure has a competitive performance, without mechanical movement or a colossal volume.

IV. CONCLUSION

This paper presented the design of a microstrip MIMO antenna configuration, based on linear antenna array elements for GB-SAR applications. The antenna accomplished 400 MHz impedance bandwidth, covering the desired bandwidth from 17.1 GHz to 17.25 GHz. Half-power beamwidths of 10° and 10 5° were achieved in the elevation and azimuth planes, respectively. A gain of 14.3 dBi and sidelobe levels of −18.5 dB for the element and −37 dB for the virtual array were realized. This configuration was validated by combining with other GB-SAR components and it showed excellent performance, making it suitable for monitoring vibrations and deformations.

REFERENCES

[1] Z. Qiu, M. Jiao, T. Jiang, and L. Zhou, "Dam structure deformation monitoring by GB-InSAR approach," *IEEE Access*, vol. 8, pp. 123287–123296, 2020.

[2] A. Karunathilake, L. Zou, K. Kikuta, M. Nishimoto, and M. Sato, "Implementation and configuration of GB-SAR for landslide monitoring: Case study in Minami-Aso, Kumamoto," *Explor. Geophys.*, vol. 50, no. 2, pp. 210–220, Apr. 2019.

[3] S. Wang and M. Sato, "A monostatic/bistatic ground-based synthetic aperture radar system for target imaging and two-dimensional displacement estimation," *IEEE Geosci. Remote Sen. Lett.*, vol. 18, no. 2, pp. 326–330, Feb. 2020.

[4] A. Karunathilake and M. Sato, "Atmospheric phase compensation in extreme weather conditions for ground-based SAR," *IEEE J. Sel. Topics Appl. Earth Observ. Remote Sens.*, vol. 13, pp. 3806–3815, Jun. 2020.

[5] H. Chai, X. Lv, and P. Xiao, "Deformation monitoring using ground-based differential SAR tomography," *IEEE Geosci. Remote Sens. Lett.*, vol. 17, no. 6, pp. 993–997, Jun. 2020.

[6] K. Takahashi, M. Matsumoto, and M. Sato, "Continuous observation of natural-disaster-affected areas using ground-based SAR interferometry," *IEEE J. Sel. Topics Appl. Earth Observ. Remote Sens.*, vol. 6, no. 3, pp. 1286–1294, Jun. 2013.

[7] H. Liu, C. Koyama, J. Zhu, Q. Liu, and M. Sato, "Post-earthquake damage inspection of wood-frame buildings by a polarimetric GB-SAR system," *Remote Sens.*, vol. 8, no. 11, pp. 1–12, 2016.

[8] S. Roedelsperger, A. Coccia, D. Vicente, C. Trampuz, and A. Meta, "The novel FastGBSAR sensor: Deformation monitoring for dike failure prediction," in *Proc. Asia–Pacific Conf. Synth. Aperture Radar (APSAR)*, Sep. 2013, pp. 420–423.

[9] G. Luzi, M. Pieraccini, D. Mecatti, L. Noferini, G. Guidi, F. Moia, and C. Atzeni, "Ground-based radar interferometry for landslides monitoring: Atmospheric and instrumental decorrelation sources on experimental data," *IEEE Trans. Geosci. Remote Sens.*, vol. 42, no. 11, pp. 2454–2466, Nov. 2004.

[10] C. Hu, J. Wang, W. Tian, T. Zeng, and R. Wang, "Design and imaging of ground-based multiple-input multiple-output synthetic aperture radar (MIMO SAR) with non-collinear arrays," *Sensors*, vol. 17, no. 3, p. 598, Mar. 2017.

[11] D. Tarchi, F. Oliveri, and P. F. Sammartino, "MIMO radar and ground-based SAR imaging systems: Equivalent approaches for remote sensing," *IEEE Trans. Geosci. Remote Sens.*, vol. 51, no. 1, pp. 425–435, Jan. 2013.

[12] F. C. Robey, S. Coutts, D. Weikle, J. C. McHarg, and K. Cuomo, "MIMO radar theory and experimental results," in *Proc. Conf. Rec. 38th Asilomar Conf. Signals, Syst. Comput.*, Pacific Grove, CA, USA, Nov. 2004, pp. 300–304.

[13] M. Pieraccini and L. Miccinesi, "An interferometric MIMO radar for bridge monitoring," *IEEE Geosci. Remote Sens. Lett.*, vol. 16, no. 9, pp. 1383–1387, Sep. 2019.

[14] M. E. Yanik and M. Torlak, "Near-field MIMO-SAR millimeter-wave imaging with sparsely sampled aperture data," *IEEE Access*, vol. 7, pp. 31801–31819, 2019.

[15] B. Zhang, F. Dai, and N. Su, "Waveform design for MIMO radar detection in a heterogeneous clutter environment," *IEEE Access*, vol. 8, pp. 86902–86914, 2020.

[16] L. Harkati, R. Abdo, S. Avrillon, and L. Ferro-Famil, "Low complexity portable MIMO radar system for the characterisation of complex environments at high resolution," *IET Radar, Sonar Navigat.*, vol. 14, no. 7, pp. 992–1000, Jul. 2020.

[17] S. Vincent, S. Francis, K. Raimond, T. Ali, and P. Kumar, "A novel planar antenna array for a ground-based synthetic aperture radar," *Serbian J. Electr. Eng.*, vol. 16, no. 2, pp. 195–209, 2019.

[18] A. S. A. El-Hameed, D. A. Salem, E. A.-F. Abdallah, and E. A. Hashish, "Quasi self-complementary UWB notched microstrip antenna for USB application," *Prog. Electromagn. Res. B*, vol. 56, pp. 185–201, 2013.
[19] A. S. Abd El-Hameed, D. A. Salem, E. A. Abdallah, H. H. Abdullah, and E. A. Hashish, "Design of dual frequency notched semicircular slot antenna with semicircular tuning stub," in *Proc. PIERS*, Aug. 2012, pp. 598–602.
[20] A. S. Abd El-Hameed, M. G. Wahab, A. Elboushi, and M. S. Elpeltagy, "Miniaturized triple band-notched quasi-self complementary fractal antenna with improved characteristics for UWB applications," *AEU-Int. J. Electron. Commun.*, vol. 108, pp. 163–171, Aug. 2019.
[21] J. Yin, Q. Wu, C. Yu, H. Wang, and W. Hong, "Low-sidelobe-level series-fed microstrip antenna array of unequal interelement spacing," *IEEE Antennas Wireless Propag. Lett.*, vol. 16, pp. 1695–1698, 2017.
[22] P. A. Dzagbletey, K. Kim, W. Byun, and Y. Jung, "Stacked microstrip linear array with highly suppressed side-lobe levels and wide bandwidth," *IET Microw., Antennas Propag.*, vol. 11, no. 1, pp. 17–22, Jan. 2017.
[23] T. Jayanthy, M. Sugadev, J. M. Ismaeel, and G. Jegan, "Design and simulation of microstrip M-patch antenna with double layer," in *Proc. Int. Conf. Recent Adv. Microw. Theory Appl.*, New Delhi, India, Nov. 2008, pp. 230–232.
[24] K. Sultan, H. Abdullah, E. Abdallah, and H. El-Hennawy, "MOM/GA-based virtual array for radar systems," *Sensors*, vol. 20, no. 3, pp. 1–16, Jan. 2020.
[25] K.-L. Wong, *Compact and Broadband Microstrip Antennas*. New York, NY, USA: Wiley, 2002.
[26] L. Kong and X. Xu, "A compact dual-band dual-polarized microstrip antenna array for MIMO-SAR applications," *IEEE Trans. Antennas Propag.*, vol. 66, no. 5, pp. 2374–2381, May 2018.
[27] A. Michelini, F. Coppi, A. Bicci, and G. Alli, "SPARX, a MIMO array for ground-based radar interferometry," *Sensors*, vol. 19, no. 2, pp. 1–11, Jan. 2019.

ANWER S. ABD EL-HAMEED (Member, IEEE) received the B.Sc. degree in electronics and communication engineering from Al-Azhar University, Egypt, in 2009, the M.Sc. degree in electronics and communication engineering from Cairo University, Egypt, in 2014, and the Ph.D. degree from the Egypt-Japan University of Science and Technology, Egypt, in May 2018. He has been working with the Microstrip Circuits Department, Electronics Research Institute, Giza, Egypt, since 2010 (on leave). He joined Kyushu University, Fukuoka, Japan, as a Special Research Student, as a part of his Ph.D. program, in June 2017. He has been a Postdoctoral Research Fellow with the Center for Northeast Asian Studies, Tohoku University, Sendai, Japan, since January 2019. His research interests include planar antennas, on-chip antennas, mm wave circuits, WPT, metamaterials, microwave imaging, archeological survey based on electromagnetic waves, and developing radar systems for cultural heritage preservation and ground surface disaster prevention. He is a Guest Editor of the Special Issue of Microwave Subsystems and Wireless Propagation in journal of *Electronics* (MDPI).

MOTOYUKI SATO (Fellow, IEEE) received the B.E., M.E., and Dr.Eng. degrees in information engineering from Tohoku University, Sendai, Japan, in 1980, 1982, and 1985, respectively. Since 1997, he has been a Professor with Tohoku University, where he was a Distinguished Professor, from 2007 to 2011, and the Director of the Center for Northeast Asian Studies, from 2009 to 2013. He was a Visiting Researcher with the Federal Institute for Geosciences and Natural Resources (BGR), Hannover, Germany, from 1988 to 1989. He was a Visiting Professor with Jilin University, China; the Delft University of Technology, The Netherlands; and the Mongolian University of Science and Technology. He developed GPR sensors for humanitarian demining, and they are used in mine affected countries, including Cambodia. His current research interests include transient electromagnetics and antennas, radar polarimetry, ground penetrating radar (GPR), borehole radar, electromagnetic induction sensing, GB-SAR, and MIMO radar systems. He was a member of the IEEE GRSS AdCom, from 2006 to 2014. He received the 2014 Frank Frischknecht Leadership Award from SEG for his contribution to his sustained and important contributions to near-surface geophysics in the field of ground-penetrating radar. He also received the IEICE Best Paper Award (Kiyasu Award) in 2017, the Achievement Award in 2019, the IEEE GRSS Education Award in 2012, and the IEEE Ulrich L. Rohde Innovative Conference Paper Awards on Antenna Measurements and Applications, in 2017. He is the Chair of the IEEE Sendai Section, from 2020 to 2021. He was an Associate Editor of IEEE Geoscience and Remote Sensing Letters, and a Guest Editor of the Special Issues on GPR2006 and GPR2010 in IEEE Transactions on Geoscience and Remote Sensing, and IGARSS2011, GPR2012, and GPR2014 of the IEEE Journal of Selected Topics in Applied Earth Observations and Remote Sensing. He was the Chair of the IEEE GRSS Japan Chapter, from 2006 to 2007. He served as the General Chair for the IGARSS2011 and the Technical Chair for the GPR1996.